

RESEARCH PAPER

Studying the Optical Properties of Nanostructure Au/TiO₂ Bi-layer Films using the SPR Technique for Biosensing Applications

Shymaa H. Saleh¹, Saeed Naif Turki Alrashid¹, Mohammed K. Khalaf^{2*}

¹ Department of Physics, College of Education for Pure Science, University of Anbar, Iraq

² Ministry of Higher Education and Scientific Research, Science and Technology, Baghdad, Iraq

ARTICLE INFO

Article History:

Received 08 September 2022

Accepted 22 December 2022

Published 01 January 2023

Keywords:

Gold

Nanostructures

Optical properties, Surface

Plasmon Sensors (SPR)

Titanium dioxide

ABSTRACT

Surface plasmon resonance (SPR) is an optical technique that can be used for sensitive optical sensor and biosensor applications. Surface plasmon resonance (SPR) biosensors consisting of alternate layers of gold (Au) and Titanium dioxide (TiO₂) thin film have been proposed as a high sensitivity property. Simulation analysis (in Matlab program) has been made for SPR of gold layer with thickness (10, 30 and 50 nm) and (TiO₂) layer with different eight thicknesses (from 10 to 100 nm), which deposited on high refractive index glasses (N_LASF9 glass prism), while the final sensing medium is the air. The analysis achieved for different wavelengths in the visible band (500-700 nm) and different refractive index (0, 0.04, 0.08 and 0.12). The properties of SPR angle θ_{SPR} have been calculated from the incident angle θ_{SPR} plot. The SPR sensitivity (S) calculated within this study. The results show that the best sensitivity and maximum sensitivity is (116.66) for thickness TiO₂=40 nm, and thickness Au =50 nm at wavelength 700 nm. for the studied refractive index.

How to cite this article

Saleh S H., Turki Alrashid S N., Khalaf M K. Studying the Optical Properties of Nanostructure Au/TiO₂ Bi-layer Films using the SPR Technique for Biosensing Applications. J Nanostruct, 13(1):8-15. DOI: 10.22052/JNS.2023.01.002

INTRODUCTION

Surface Plasmon Resonance (SPR) property appears on the surfaces of some metals and is the result of the collective movement of free electrons present in the nanoparticle when light falls on them [1]. The SPR occurs when polarized light hits an electrically conductive surface at the interface between two media, and thus this generates charge density waves of electrons called plasmons, which leads to a reduction in the intensity of the reflected light at a certain angle called the angle of resonance [2]. When considering optical properties of thin metal films surface plasmon technique is widely used. [3-5]. The material (TiO₂) Titanium oxide is one of the minerals that have

great importance in optical applications because it has many optical properties [6]. In addition to the transmittance to the visible and far-infrared range of the electromagnetic spectrum [7]. Films manufactured from these oxides are highly durable and have a high refractive index, so they are suitable for applications of anti-reflective coatings and multi-layer optical coatings [8]. In (2015) Borges, J., used TiO₂/Au thin films to study the physical and chemical properties of proteins, whereby a TiO₂/Au membrane was prepared and then heat treated. Au by a DC magnetic splatter method was detected and the membrane efficiency was 8.3%, at a temperature of 300°C, and 500°C [9]. In (2016) researchers DINGYI FENG

* Corresponding Author Email: mohammedkhkh@yahoo.com



This work is licensed under the Creative Commons Attribution 4.0 International License.

To view a copy of this license, visit <http://creativecommons.org/licenses/by/4.0/>.

used gold-coated fiber of infrared wavelengths to make a Tilted fiber Bragg gratings (TFBG) sensor and used a single- and double-sided tilt angle. 50 layers of gold were deposited with a thickness of nanometers; the experimental results show the similarity of the TFBG-SPR sensors with perfectly uniform precipitation-based processes. One of the precipitation conditions is that the precipitates are oriented appropriately in the direction of the tilt level, and this is considered difficult to apply, as it must be within 5 nanometers. [10]. In (2017) Md. R. Hasan et al proposed numerically demonstrate a two-layer circular lattice photonic crystal fiber (PCF) biosensor based on the principle of surface plasmon resonance (SPR). The finite element method (FEM) with circular perfectly matched layer (PML) boundary condition is applied to evaluate the performance of the proposed sensor. A thin gold layer is deposited outside the PCF structure, which acts as the plasmonic material for this design [11]. In (2020) Keyi Li et al proposed a different surface plasmon resonance biosensor by incorporating emerging two-dimensional material blue phosphorus and graphene layers with plasmonic gold film theoretically. They can provide sensitivity up to 1.4731×10^5 °/RIU, [12]. In (2021) Farah J. et al proposed an optical sensing applications and biosensors. Simulation analysis (using Matlab) has been done for SPR for gold (Au) layer with thickness (40 nm) and Polyvinyl Alcohol (PVA) polymer with various thickness (10, 20, 30, 40, 50, 60, 70 and 80 nm) deposited on glass prism type D-ZLAF50_Dense lanthanum flint. The

analysis was taken for different wavelengths from ultra- violet of wavelength 100 nm to near infra- red wavelength of 1000 nm. The SPR sensitivity (S) was calculated. The maximum obtained sensitivity was 207.5 for (PVA) thickness of 30 nm and 40 nm, $\Delta n = 0.08$ at wavelength 800 nm and 1000 nm, respectively. The best sensitivity in visible region (700 nm) was 158.33 for thickness 20 nm, $\Delta n = 0.12$. [13].

In this study a simulation program was constructed in Matlab Program by adopting the Fresnel equations of reflectivity of electromagnetic waves in range Visible and using the transfer matrix for a system consisting of a semicircular prism on which two layers were deposited: The second is TiO₂ with a thickness of (10-100 nm) and the first is gold with a variable thickness started (10 nm, 30 nm, 50 nm, 80 nm). The simulations were presented to prompt a determination to understand the shape of the resonances when the sensor head (gold thin film) biosensor was applied as a pollutant gas.

MATERIALS AND METHODS

Electromagnetic waves at metal dielectric interfaces

To find the state that allows the presence of a surface electromagnetic wave propagating at the interface between two different media. We consider two semi-infinite media with complex dielectric functions M_1 and M_2 divided by a planar interface parallel to the x direction as is represented in Fig. 1. Each of the electromagnetic

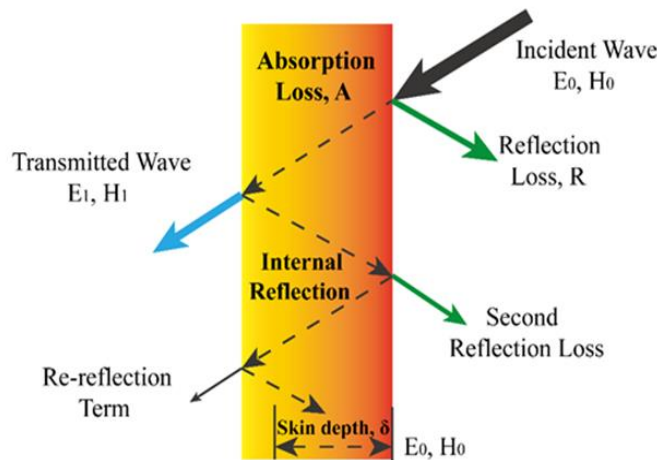


Fig. 1. The interface between two semi-infinite mediums is demonstrated. It's worth noting that the electromagnetic field is TM polarized [15].



fields must satisfy Maxwell's equations and the boundary conditions for electromagnetic fields. It is necessary to consider two different possible states of polarization of the electromagnetic wave: transverse magnetic wave (TM) and transverse electric wave (TE), where the magnetic field or the electric field is respectively perpendicular to the plane of incidence [14].

(a) *Transverse Magnetic (TM) polarization*

While we look for traveling, electromagnetic waves for easy way Expression the fields in the two semi-infinite media is the following. [16]:

$$E_j = (E_x, j, 0, E_z) \exp(i(M_x, j_x + M_z, j_z) - i\omega t) \quad (1)$$

$$H_j = (0, H_y, j, 0) \exp(i(M_x, j_x + M_z, j_z) - j\omega t) \quad (2)$$

Where j= 1, 2.

The dispersion relation of the surface Plasmon is [16]:

$$\beta = \frac{\omega}{c} \sqrt{\frac{\epsilon_1 \epsilon_2}{\epsilon_1 + \epsilon_2}} \quad (3)$$

The expression for the normal component of the wave vector obtained [16].

$$M_{j,Z} = \frac{\omega}{C} \sqrt{\frac{\epsilon_1^2}{\epsilon_1 + \epsilon_2}} \quad (4)$$

That β is called propagation constant and M is the wave vector, ϵ_1 and ϵ_2 of dielectric material and metal, respectively. Is the light angular frequency, C is the speed of light.

(b) *Transverse Electric TE polarization*

Since we are looking for magnetic field is parallel to the incidence plane, the boundary conditions and Maxwell's equation lead to the relations [17]:

$$M_{z_{01}} + M_{z_{02}} = 0, \quad (5)$$

$$M_{x,1} = M_{x,2} \quad (6)$$

That, together lead for equation [17]:

$$M_1^2 = \left(\frac{\omega}{C}\right)^2 M_1 \quad (7)$$

$$M_2^2 = \left(\frac{\omega}{C}\right)^2 M_2 \quad (8)$$

Methodology: Measurement of the optical constants of Au and TiO₂ layers

The Simulation analysis (in Matlab) consists of four media, such as glass prism (half-sphere type N-LASF9_glass), deposited on it layer of gold with the thickness (10, 30, 50) nm, and TiO₂ with different thickness from (10 to100) nm step10 nm with the final medium (sensing polluting gases), using the excitation light beam different wavelengths from 500 to 700 nm (Fig. 2).

The wave vector of the surface plasma wave suffers a perturbation ΔM respect to the wave vector β . The dispersion relation of the surface plasmon, is [18]:

$$\beta = \frac{\omega}{c} \sqrt{\frac{\epsilon_1 \epsilon_2}{\epsilon_1 + \epsilon_2}} = \beta' + \beta'' \quad (9)$$

, since ω is the light angular frequency, c is the speed of light, ϵ_1 and ϵ_2 are the complex dielectric functions for medium1 and medium2 respectively . So β characteristic of two semi-infinite media, and can be written. [18]:

$$\beta' = \beta + \Delta M \quad (10)$$

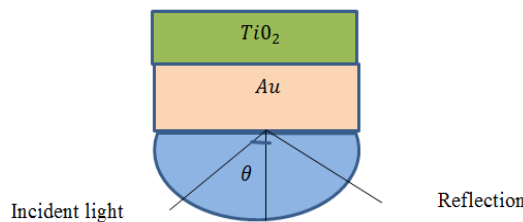


Fig. 2. Schematic diagram of the proposed SPR sensor (Au and TiO₂)

That real part of ΔM causes a displacement of the resonance position compared to $\text{Re}(\beta)$, while its imaginary part is related with the presence of the prism and the finite thickness of the metal layer. This new term ΔM can be approximated as the contribution of the intrinsic damping, which represents the joule loss in the metal, and the radiation damping which represents the energy lost by back-coupled radiation. For metals generally used in SPR experiments such as aluminum, gold or silver, it exists an analytic approximation of the SPR curve near the angle of resonance θ_{SPR} which is given by [19]:

$$R = 1 - \frac{4I_m(\beta)I_m(M)}{n^2M^2(\sin\theta - \sin\theta_{\text{SPR}}) + I_m(\beta r)^2} \quad (11)$$

And I_m is imaginary part and M_0 the vacuum of wave vector, surface Plasmon resonance is the requires wave vector of the incident light in the plane of the surface (M_x) match the wave vector of the SP wave in metallic films M_{SP} [20]:

$$M_x = n_p \left(\frac{2\pi}{\lambda} \right) \sin\theta \quad (12)$$

$$M_{\text{SP}} = \frac{2\pi}{\lambda} \sqrt{\frac{\epsilon_1\epsilon_2}{\epsilon_1 + \epsilon_2}} \quad (13)$$

M_1 and M_2 represent complex dielectric constant of dielectric material and metal, respectively.

n_p : is the refractive index of the prism. λ and θ : are wavelength and angle of incident light, respectively. The matching relationships for SPR are $M_x = M_{\text{SP}}$ [20] where

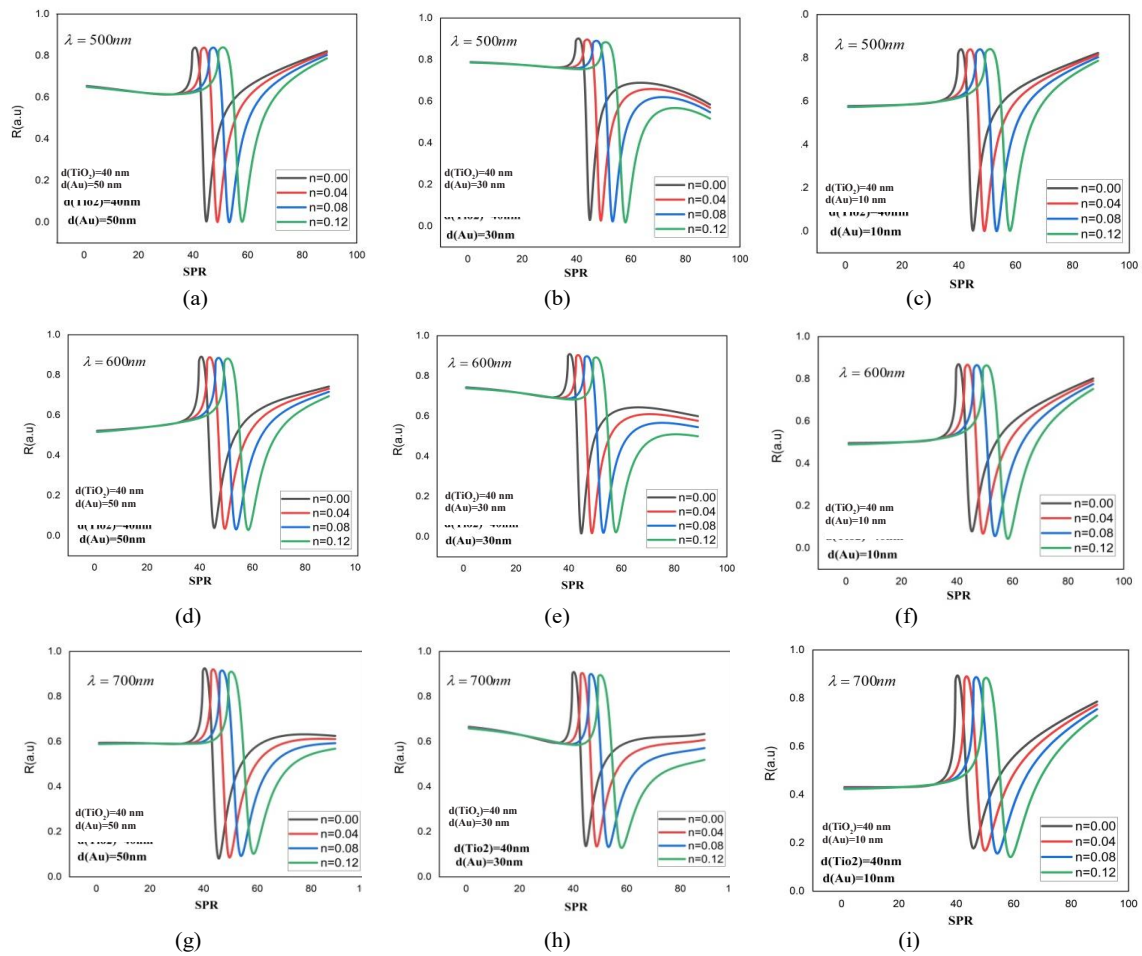


Fig. 3. The relation between reflectance with incident angle for different thickness TiO₂ and wavelength (λ) = 500, 600 and 700 nm.

$$\theta_{SPR} = \sin^{-1} \sqrt{\frac{M_1 M_2}{M_2(M_1 + M_2)}} \quad (14)$$

Where the resonant angle is can be adjusted by controlling the angle of incidence in order to match the propagation constant of the plasmon waves and the sensitivity of the sensor to changes in the refractive index of an analyte placed in direct contact with the sensor surface is defined by [13]:

$$S_n = \frac{\partial \theta_{SPR}}{\partial n} \quad (15)$$

where θ_{SPR} is the resonant angle, =how that for wavelengths of electromagnetic waves in the visible range, and using noble metals such as gold the ratio of the losses terms reaches 1 when the thickness is approximately 50 nm. Further, it is possible to demonstrate that the full width half

maximum (FWHM) of the curve of reflectivity is proportional to the imaginary part of the wave vector of the plasma wave, that is to the losses of the systems [13].

RESULTS AND DISCUSSION

The film thickness of a single metal-based SPR sensor has to be such that the resonance curve produced by a sensor structure under consideration not only shows the maximum possible loss in reflectivity and absorption but also produces the slimmest possible FWHM of the reflectivity curve. The thickness range for a gold film-based SPR sensor would be (10, 30, and 50) nm. Fig. 3a, b, c, d, e, f, g, h and i show the relationship between reflectivity as a function of the angle of incidence of the light ray. Where shown that the SPR curves resulting from the simulation of the proposed system consisted of a gold layer and a titanium layer for different states

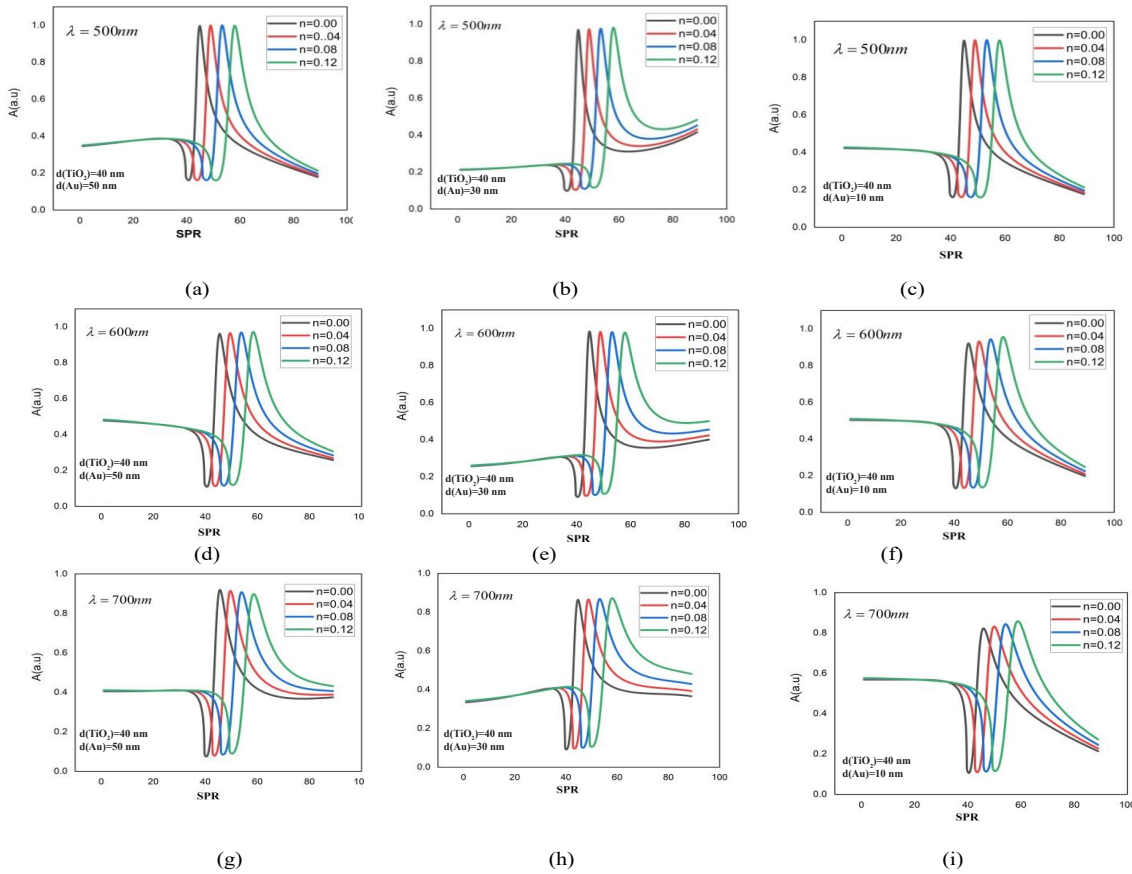


Fig. 4. The relation between absorption with incident angle for different thickness TiO₂ and wavelength (λ) = 500, 600 and 700 nm.



of titanium thicknesses and different wavelengths. Any minimum reflectivity value corresponds to the maximum energy loss due to the high absorption of the light beam within the sensor system. The excitation of the surface plasmon is determined by the angle of resonance of the surface plasmon. The surface plasmon resonance revealed by the curves in this figure can be determined as follows There is SPR at $\lambda= 500$ nm for TiO₂ thickness is 40 nm and Au thicknesses are (10,30,50 nm) ,The best SPR at Au thickness $d=50$ nm in $\lambda= 500$ nm see Fig. 3a, b and c. There is SPR at $\lambda=600$ nm for TiO₂ thickness is 40 nm and Au thicknesses are (10, 30, 50 nm). The best SPR at Au thickness $d=30$ nm in $\lambda=600$ nm see Fig. 3d, e and f. There is SPR at $\lambda=700$ nm for TiO₂ thickness is 40 nm and Au thicknesses are (10, 30, 50 nm), the best SPR at Au thickness $d=50$ nm in $\lambda=700$ nm see Fig. 3g, h and i. The surface Plasmon resonance angle (θ_{spr}) shifts to a higher angle when $\lambda=500$ nm especially at TiO₂ thicknesses 40 nm and Au 50 nm.

Fig. 4a, b, c, d, e, f, g, h and i shows the

relationship between absorption as a function of the angle of incidence of the light ray. Where shown that the SPR curves resulting from the simulation of the proposed system consisting of a gold layer and a TiO₂ layer for different states of titanium thicknesses and different wavelengths. Any maximum value of absorption corresponds to the minimum energy loss due to the Low absorption of the light beam within the sensor system. The excitation of the surface plasmon and is determined by the angle of resonance of the surface plasmon. The surface Plasmon resonance revealed by the curves in this figure can be determined as follows. There is SPR at $\lambda= 500$ nm for TiO₂ thickness is 40 nm and Au thicknesses are (10, 30, 50 nm). The best SPR at Au thickness $d= 50$ nm in $\lambda= 500$ nm see Fig. 4a, b and c. There is SPR at $\lambda= 600$ nm for TiO₂ thickness is 40 nm and Au thicknesses are (10, 30,50 nm) .The best SPR at Au thickness $d= 30$ nm in $\lambda=600$ nm see Fig. 4d, e and f. There is SPR at $\lambda=700$ nm for TiO₂ thickness is 40 nm and Au thicknesses are (10, 30,50 nm)

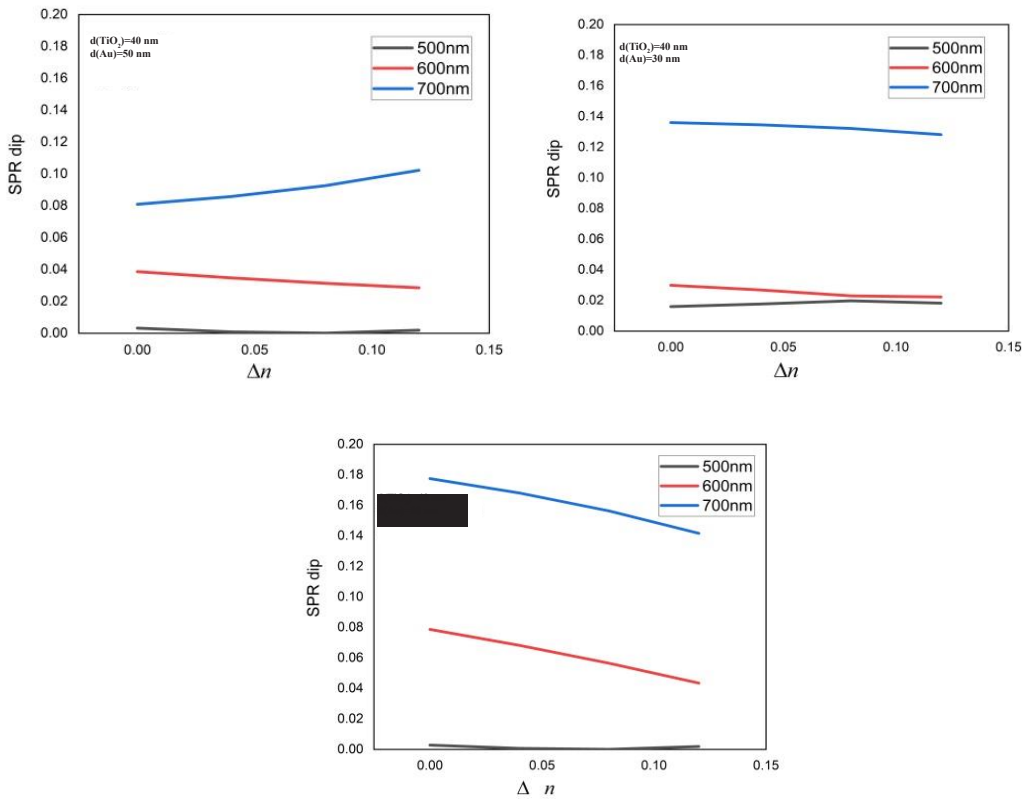


Fig. 5. The variation of SPR dip length (Ld) with the change of refractive index of layers for different thickness (Au) and wavelength (500,600,700 nm.)

.The best SPR at Au thickness $d=50$ nm in $\lambda=700$ nm seeing Fig. 4g, h and i.

The surface Plasmon resonance angle (θ_{SPR}) shifts to a higher angle when $\lambda=500$ nm especially at TiO₂ thicknesses 40 nm and Au 50 nm.

The properties of SPR dip length (L_d) against the changing of the refractive index of sensing medium increased length are shown in Fig. 5. It has been noted that the decreased plasmonic bottom length (SPR dip length) with increased TiO₂ thickness at the wavelengths 500, 600, and 700 nm. It is noticed that there is an observable increase in the length when increasing the wavelength from 500, 600 to 700 nm at the same thickness of TiO₂, meaning a further improvement in the plasmonic resonance.

On the other hand, Fig. 3 Illustrated the relation between reflectance with incident angle, that once the thickness increases from (10-100) nm, the dip of SPR all thickness of TiO₂ layers appear and become sharper at 500 nm. Also, Fig. 4 Illustrates the relation between absorption with incident angle, that once the thickness increases from (10-100) nm, the dip of SPR for all thicknesses of TiO₂ layers becomes severer at 500 nm.

Table1, it shows the sensitivity values and thicknesses for two layers of TiO₂ and Au within the visible range. The best result of sensitivity at thickness of ($d=40$ nm) for TiO₂ when using wavelength 500-700 nm and thickness of Au ($d=50$ nm) at wavelength 700 nm.

CONCLUSION

In summary, differences in the performance of SPR sensing to prism-based for Au layer (10, 30,50 nm) following the addition of the layers of TiO₂ (10-100 nm) were investigated in this paper. The performance of the Au/TiO₂ layers was analyzed and numerically simulated. Finally, the sensitivity and the properties of θ_{SPR} calculated from curve reflectance with incident angle θ_{incid} for each structure were obtained via simulations involving changes in the refractive index of the sensitive layer. Numerical simulation results showed the following points; the biosensor Au-TiO₂ layer deposited on prism gave SPR dip at wavelength 500,600 and 700 nm and shows no appearance for wavelength 500 in the viable range. The best SPR is in the wavelength 500 nm at TiO₂ thickness $d=40$ nm, Au thickness $d=50$ nm at $\Delta n=0.12$ and for the wavelength 600nm, TiO₂ thickness at $d=40$ nm. Au thickness $d=50$ nm at $\Delta n=0$. The findings of

this work can be used as a theoretical foundation for making major adjustments to SPR sensors to improve their sensitivity.

The best result of sensitivity at thickness of ($d=40$ nm) for TiO₂ when using wavelength 500-700 nm and thickness of Au ($d=50$ nm) at wavelength 700 nm.

CONFLICTS OF INTEREST

The authors declare that there is no conflict of interests regarding the publication of this manuscript.

REFERENCES

1. Awad HD, Khalaf MK, Abd Algaffar AN. Noble Metal Thin Film Thickness Optimization for Sharp Surface Plasmon Resonance Reflectance Curve. *Mater Sci Forum*. 2021;1039:442-450.
2. Zeng S, Baillargeat D, Ho H-P, Yong K-T. Nanomaterials enhanced surface plasmon resonance for biological and chemical sensing applications. *Chem Soc Rev*. 2014;43(10):3426.
3. van Exter M, Lagendijk A. Ultrashort Surface-Plasmon and Phonon Dynamics. *Phys Rev Lett*. 1988;60(1):49-52.
4. Groeneveld R, Sprik R, Lagendijk A. Ultrafast relaxation of electrons probed by surface plasmons at a thin silver film. *Phys Rev Lett*. 1990;64(7):784-787.
5. Temnov VV. Ultrafast acousto-magneto-plasmonics. *Nature Photonics*. 2012;6(11):728-736.
6. Khalaf MK, Roomy HM, Oraibi NS. Structural and optical properties of TiO₂ single layer and Bi-layered Ag/TiO₂ prepared by DC/RF magnetron sputtering. *AIP Conf Proc: AIP Publishing*; 2021.
7. Guo Q, Arnoux C, Palmer RE. <title>Fabrication of micro/nanostructured surfaces using self-organized processes</title>. *BioMEMS and Smart Nanostructures*; 2001/11/19: SPIE; 2001.
8. Li M, Su J, Guo L. Preparation and characterization of ZnIn₂S₄ thin films deposited by spray pyrolysis for hydrogen production. *Int J Hydrogen Energy*. 2008;33(12):2891-2896.
9. Borges J, Costa D, Antunes E, Lopes C, Rodrigues MS, Apreutesei M, et al. Biological behaviour of thin films consisting of Au nanoparticles dispersed in a TiO₂ dielectric matrix. *Vacuum*. 2015;122:360-368.
10. Feng D, Zhou W, Qiao X, Albert J. High resolution fiber optic surface plasmon resonance sensors with single-sided gold coatings. *Opt Express*. 2016;24(15):16456.
11. Hasan M, Akter S, Rifat A, Rana S, Ali S. A Highly Sensitive Gold-Coated Photonic Crystal Fiber Biosensor Based on Surface Plasmon Resonance. *Photonics*. 2017;4(4):18.
12. Li K, Li L, Xu N, Peng X, Zhou Y, Yuan Y, et al. Ultrasensitive Surface Plasmon Resonance Biosensor Using Blue Phosphorus-Graphene Architecture. *Sensors*. 2020;20(11):3326.
13. Kadhun FJ, Saeed AA, Al-kadhemy MFH, Al-Zuky AAD, Al- Saleh AH. Theoretical Biosensor Design for Gold- PVA Surface Plasmon Resonance Layers. *Iraqi Journal of Science*. 2021:4232-4239.
14. Raether H. Surface plasmons on gratings. *Springer Tracts in Modern Physics: Springer Berlin Heidelberg*; 1988. p. 91-

- 116.
15. Zhao B, Zhang R. Electromagnetic Wave Absorption Properties of Core-Shell Ni-Based Composites. *Electromagnetic Materials and Devices*: IntechOpen; 2020.
16. Aubry A, Lei DY, Maier SA, Pendry JB. Interaction between Plasmonic Nanoparticles Revisited with Transformation Optics. *Phys Rev Lett*. 2010;105(23).
17. Qi L, Yang Z, Lan F, Gao X, Shi Z. Properties of obliquely incident electromagnetic wave in one-dimensional magnetized plasma photonic crystals. *Physics of Plasmas*. 2010;17(4):042501.
18. Gutiérrez Rodrigo S. Study of the optical properties of nano-structural metallic systems with the Finite-Difference Time-Domain method Sergio. *Prensas Universitarias de Zaragoza*; 2010.
19. Rouf HK, Haque T. PERFORMANCE ENHANCEMENT OF AG-AU BIMETALLIC SURFACE PLASMON RESONANCE BIOSENSOR USING INP. *Progress In Electromagnetics Research M*. 2018;76:31-42.
20. Huang X, El-Sayed MA. Gold nanoparticles: Optical properties and implementations in cancer diagnosis and photothermal therapy. *Journal of Advanced Research*. 2010;1(1):13-28.